Conformational Transition between Native and Reactive Center Cleaved Forms of α_1-Antitrypsin by Fourier Transform Infrared Spectroscopy and Small-Angle Neutron Scattering

Parvez I. Haris,[‡] Dennis Chapman,[‡] Richard A. Harrison,[§] Kathryn F. Smith,[‡,∥] and Stephen J. Perkins*[,‡,∥]

Departments of Protein and Molecular Biology and of Biochemistry and Chemistry, Royal Free Hospital School of Medicine, Rowland Hill Street, London NW3 2PF, U.K., and Molecular Immunopathology Unit, MRC Centre, Hills Road, Cambridge CB2 2QH, U.K.

Received November 1, 1989; Revised Manuscript Received December 12, 1989

ABSTRACT: α_1-Antitrypsin (α_1-AT) is the best-characterized member of the serpin superfamily of plasma proteins. Protease inhibitor members of this family undergo a characteristic reactive-center cleavage during expression of their inhibitory activity. The physical basis of this transition in α_1-AT from the stressed native conformation to the more stable reactive center cleaved (split) form was studied by Fourier transform infrared (FT-IR) spectroscopy and neutron scattering. The FT-IR spectra show that, while split α_1-AT has three intense well-resolved components associated with the presence of antiparallel β-sheet and α-helix conformations, the amide I band of native α_1-AT has only one intense component, associated with the presence of β-sheet structure. ^1H–^2H exchange within the polypeptide backbone, studied by FT-IR and NMR spectroscopy, shows that the native form undergoes greater exchange than the split form. Under the same conditions, neutron scattering shows no differences in the radius of gyration R_G of the native and the split forms. In contrast, in high concentrations of phosphate approaching those used for crystallization, the native form (unlike the split form) undergoes dimerization. These data indicate that the conformational transition largely involves localized secondary and tertiary structure rearrangements. We propose that the energetically stressed native α_1-AT structure is the consequence of a significantly reduced number of hydrogen bonds in secondary structure components and that reactive-site cleavage between Met358 and Ser359 is the key for the development of the fully hydrogen bonded more stable serpin structure.

Members of the serpin superfamily, which includes many plasma proteinase inhibitors, present a reactive site as an ideal substrate to the target proteinase (Carrell & Travis, 1985). After reaction, a stable stoichiometric 1:1 complex between proteinase and reactive center cleaved (split) inhibitor is formed. The crystal structure of a reactive center cleaved form of α_1-AT shows that on cleavage a significant conformational change must occur, since the newly formed termini at Met358 and Ser359 are 7 nm apart (Löbermann et al., 1984). Despite this, details of the physicochemical basis of the improved stability of the split form (Carrell & Owen, 1985) remain unclear.

We report here Fourier transform infrared (FT-IR) spectroscopy (Lee & Chapman, 1986; Susi & Byler, 1986; Surewicz & Mantsch, 1988) and small-angle neutron scattering (Perkins, 1988a,b) studies of α_1-AT. These are complementary techniques that examine the polypeptide backbone conformation and the gross structure of α_1-AT in solution, both under conditions close to physiological and to those of the crystal structure (2.6 M phosphate). FT-IR spectroscopy has advantages over circular dichroism for the study of secondary structures since there is no problem in defining a base line in the FT-IR spectrum, different parts of the FT-IR spectrum can be clearly resolved, and information is provided on amide proton exchange rates in proteins. Neutron scattering rather than X-ray scattering is more advantageous, since the sample transmission in 100% ^2H_2O (2-mm path length) is reduced by only 3% in 1.8 M phosphate relative to 0.05 M phosphate, while the reduction for X-rays (1-mm path length) is 81% in 1.2 M phosphate. The combined use of both techniques places limits on the structural changes seen between the two forms of α_1-AT and leads to the proposal of a mechanism by which the split form of α_1-AT is stabilized.

Materials and Methods

The preparation of α_1-AT and the characterization of the samples is described in Smith et al. (1990). The FT-IR, NMR, and neutron samples were dialyzed over 36 h into sodium potassium phosphate buffers ranging from 0.05 to 1.80 M in 100% ^2H_2O at 6 °C with four changes of buffers.

Infrared spectra were recorded on a Perkin-Elmer 1750 Fourier transform infrared spectrometer equipped with a TGS detector. A Perkin-Elmer Model 7300 data station was used for data acquisition, storage, and analysis. Spectral conditions [defined more fully in Haris et al. (1986) and Perkins et al. (1988)] were as follows: α_1-AT concentration 23–25 mg/mL on the basis of an A_{280} (1%, 1 cm) of 5.4; 400 scans (1-h accumulation); spectral resolution 4 cm^{-1}; sample thickness of 50 μm using a Teflon spacer. Spectral deconvolution was performed with the Perkin-Elmer ENHANCE function (Haris et al., 1986), which is analogous to the method developed by Kauppinen et al. (1981), using deconvolution parameters of $\sigma = 8$ (half-width at half-height) and $k = 2.25$. The second-derivative spectra were calculated over a 13-cm^{-1} range.

Neutron scattering data were measured at 20 °C on the small-angle scattering instrument D17 at the Institut Laue Langevin, Grenoble, with a wavelength λ of 1.105 nm

* To whom correspondence should be addressed at the Department of Biochemistry and Chemistry.

‡ Department of Protein and Molecular Biology, Royal Free Hospital School of Medicine.

§ MRC Centre.

∥ Department of Biochemistry and Chemistry, Royal Free Hospital School of Medicine.

0006-2960/90/0429-1377$02.50/0

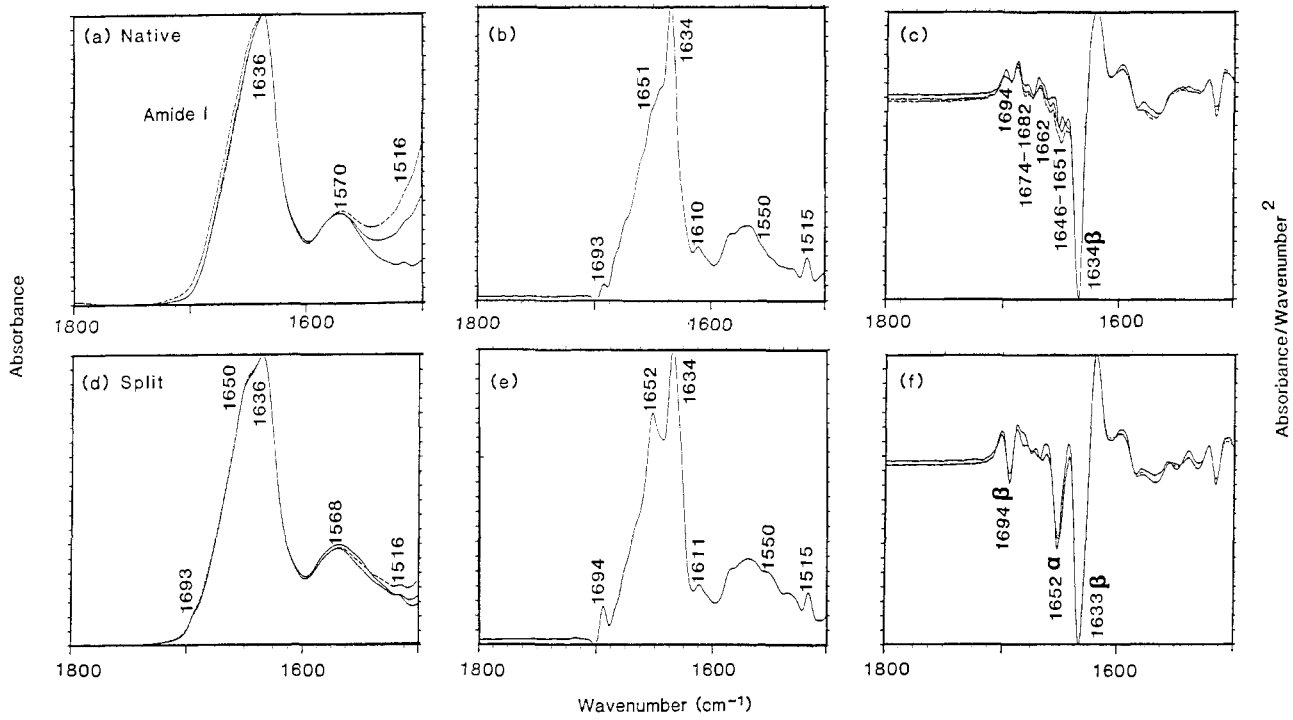

FIGURE 1: Fourier transform infrared spectroscopy of native and split α_1-AT. Panels a, b, and c correspond to the absorbance, deconvoluted, and second-derivative spectra of native α_1-AT in that order; panels d, e, and f correspond likewise to split α_1-AT. The absorbance and second-derivative spectra are shown for samples recorded in 0.05 (—), 0.50 (—), and 1.25 M (---) sodium potassium phosphate buffers in ^2H_2O at 20 °C. The increase in signal intensity at 1500 cm^{-1} for native α_1-AT in 0.50 and 1.25 M phosphate buffers is attributed to the presence of trace amounts of $^1HO^2H$. The deconvoluted spectra were recorded in 0.05 M sodium potassium phosphate buffers; the peaks are not fully labeled for reason of clarity but are similar to those in the second-derivative spectra.

(wavelength spread $\Delta\lambda/\lambda$ of 10%) and a sample-detector distance of 3.396 m to correspond to a Q range of 0.07–0.60 nm^{-1} ($Q = 4\pi \sin\theta/\lambda$; 2θ = scattering angle). Data collection employed 2 mm thick Hellma cells. Analyses followed standard procedures, which utilized backgrounds based on the scattering of the buffer dialyzate, cadmium, H_2O, and an empty Hellma quartz cell and measurements of sample and buffer transmissions (Ghosh, 1989; Perkins et al., 1990; Smith et al., 1990). The radius of gyration R_G and the forward scattering at zero scattering angle $I(0)$ were determined from plots of ln $I(Q)$ vs Q^2 with the Guinier equation (Glatter & Kratky, 1982): ln $I(Q)$ = ln $I(0) - R_G^2Q^2/3$ in the Q range 0.15–0.58 nm^{-1} except for native α_1-AT above 1.2 M phosphate, where it was 0.15–0.41 nm^{-1}.

Results and Discussion

Panels a and d of Figure 1 show the Fourier transform infrared spectra of native and split α_1-AT. The amide I maxima in both cases is centered at 1636 cm^{-1}. The feature at 1568–1570 cm^{-1} corresponds to absorption from carboxylate side chains. The 1516-cm^{-1} component is normally attributed to tyrosine side chain absorption. The frequency of the main amide I band for both samples is consistent with the presence of a predominantly β-sheet structure in α_1-AT (Surewicz & Mantsch, 1988; Haris et al., 1986). However, native and split α_1-AT differ in that additional features near 1650 and 1693 cm^{-1} are present in the split form. These were reproducibly observed in 0.05, 0.50, and 1.25 M phosphate (and also in 0.80, 1.60, and 1.80 M phosphate; not shown). The second-derivative spectra of the two forms in panels c and f of Figure 1 emphasize the differences more clearly. The main β-sheet feature at 1633–1634 cm^{-1} is visible in both forms. The split form shows considerably more intense β-sheet and α-helix bands at 1694 and 1652 cm^{-1}, and the band at 1633 cm^{-1} is broader. The bands near 1650 and 1690 cm^{-1} have been attributed to α-helix and antiparallel β-sheet structures, respectively (Haris et al., 1986; Olinger et al., 1986). For both native and split α_1-AT, similar weaker features were generally observed near 1646, 1662, and 1674–1682 cm^{-1}. The feature visible in the native form near 1646 cm^{-1} most likely corresponds to disordered structures. Those near 1662 and 1674–1682 cm^{-1} probably correspond to turn structures, although overlap from β-sheet and 3_{10} helices may also occur. The use of deconvolution for resolution enhancement led to very similar results (Figure 1b,e).

The FT-IR spectroscopic results clearly show that the α-helical and antiparallel β-sheet content has significantly increased after reactive-site cleavage of α_1-AT. Methods for the quantitative assessment of the differences seen between the two forms of α_1-AT by curve fitting of the amide I band are however insufficiently accurate at the present time (Mantsch et al., 1989). Inspection of the crystal structure of split α_1-AT (32% α-helix; 40% β-sheet) suggests that in native α_1-AT strand A4 is withdrawn from β-sheet A (Löbermann et al., 1984). The formation of about 20–30 additional hydrogen bonds in the largely antiparallel β-sheet A of split α_1-AT would account for the appearance of the band at 1694 cm^{-1}. The increase in α-helix content after cleavage is however unexpected. In the crystal structure, in linear sequence, helices A and B flank strand B6, helices D, E, and F alternate with strands A2, A1 and A3, and helices H and I flank strand A6. The infrared data suggest that in the native molecule either these helices are not formed or they are considerably distorted along their length at the same time that β-sheet A is incompletely formed. Thus, after reactive-site cleavage, a concerted drive toward the formation of stable, fully hydrogen bonded α-helix and β-sheet structures results in a molecule (split α_1-AT) of increased stability.

The intensity of the amide II band at 1552 cm^{-1} monitors the residual ^1H–^2H exchange of backbone NH protons. Panels

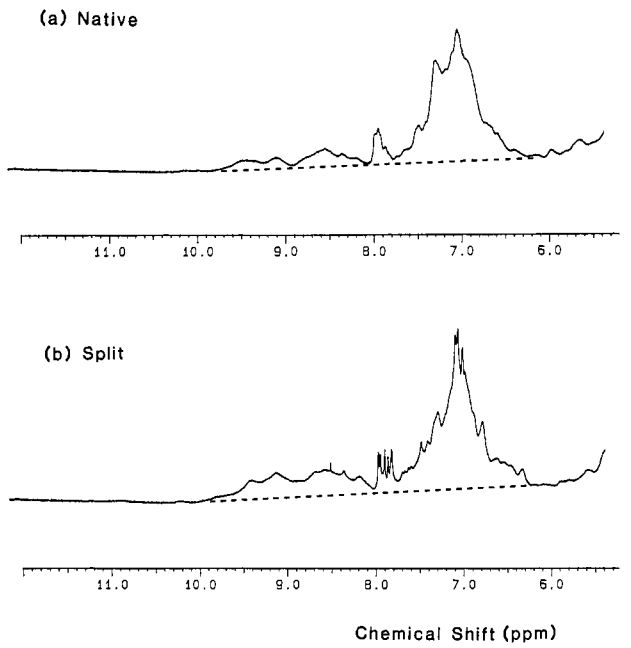

FIGURE 2: 400-MHz ^1H NMR spectra of native and split α_1-AT at 30 °C in 0.05 M sodium potassium phosphate buffers in ^2H_2O (concentrations 23–25 mg/mL). The downfield region is shown, with the chemical shift scale set relative to the $^1HO^2H$ signal at 4.695 ppm downfield of (trimethylsilyl)propionic acid. The aromatic proton signals from 27 Phe, 13 His, 6 Tyr, and 2 Trp residues were assigned to the envelope between 6.3 and 8.0 ppm and the amide proton signals to that between 8.0 and 9.9 ppm. 256 scans were recorded with water decoupling and 3 s between pulses. The spectral resolution was improved with a sine bell squared routine.

a and d of Figure 1 show that, after identical, simultaneous dialysis into ^2H_2O, this is 15% lower for the native form than for the split form. In the deconvoluted spectra of Figure 1b,e, a peak at 1550 cm^{-1} is visible for split α_1-AT but not for native α_1-AT. These indicate that ^1H–^2H exchange is more extensive in the native form, as might be expected for a more open structure. This was confirmed by 400-MHz ^1H NMR spectroscopy (Figure 2) on the same samples used in Figure 1b,e. Integration of the spectra downfield of the 195 aromatic proton signals shows that while 11% of the 377 NH protons are nonexchanged in native α_1-AT this increases to 19% in split α_1-AT. The greater exchange in native α_1-AT is consistent with a reduced content of ordered secondary structures. [Other NMR spectral differences between the two forms include the observation of narrower line widths in split α_1-AT (Figure 2) and rearranged patterns in the ring current shifted methyl proton signals at the high-field end of the spectra. Both of these are consistent with the existence of structural and dynamic differences between the two forms of α_1-AT.]

The magnitude of the observed changes in backbone structure (Figure 1; Bruch et al., 1988) suggests that native and split α_1-AT may have different gross structures. This was investigated by small-angle neutron scattering. The R_G and $I(0)/c$ Guinier parameters from dilution series are dependent on α_1-AT concentrations c between 0.05 and 0.50 M phosphate. The values after extrapolation to zero c are shown in Figure 3. No difference could be detected between the native and split forms of α_1-AT up to 0.80 M phosphate, even though for other proteins such as hemoglobin (Conrad et al., 1969), aspartate transcarbamylase (Moody et al., 1979), and hexokinase (McDonald et al., 1979) the appropriate conformational changes after ligation are detectable from Guinier analyses. The folded tertiary structures of native and split α_1-AT are thus essentially similar, and this places an upper limit on the structural changes in the polypeptide backbone indicated by

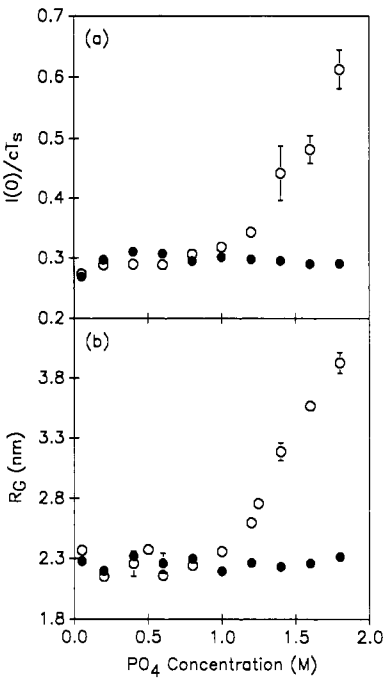

FIGURE 3: Summary of neutron Guinier R_G and $I(0)$ analyses of native (○) and split (●) α_1-AT in ^2H_2O buffers. (a) Dependence of $I(0)/cT_s$ on phosphate concentration after extrapolation of $I(0)/cT_s$ to zero concentration in each buffer (c, α_1-AT concentration; T_s, sample transmission). Between three and six measurements were made at each phosphate concentration in a range of c of 3–12 mg/mL. (b) Corresponding R_G values after extrapolation to zero concentration.

FT-IR, circular dichroism (CD), and NMR spectroscopy (Smith et al., 1990).

Final experiments were performed at high phosphate concentrations approaching those used for crystallization. The FT-IR data in 1.25 M (Figure 1), 1.60 M, and 1.80 M phosphate show no significant difference from those in 0.05 M, 0.50 M (Figure 1), and 0.80 M phosphate. However, the neutron data (Figure 3) show that above 1 M phosphate the $I(0)/c$ data rise to double the low-phosphate values for native α_1-AT but are unchanged for the split form. This shows that native α_1-AT forms dimers in 1.8 M phosphate. The corresponding R_G data for native α_1-AT rise in parallel. While the structure of split α_1-AT is unaffected by high phosphate, the association of native α_1-AT indicates that the surface properties of several amino acid residues are significantly different.

Conclusions

Neutron scattering shows that under physiological conditions the gross folded structures of native and split α_1-AT are similar. However, within the secondary and tertiary structures of both forms of α_1-AT, subtle but marked structural differences were identified by use of FT-IR spectroscopy and neutron scattering. CD and NMR spectroscopic studies (Figure 2; Bruch et al., 1988; Gettins & Harten, 1988) have also shown that there are conformational differences between the native and split forms of other members of the serpin superfamily. These data are supported by monoclonal antibodies with different epitopic specificities which bind either to native or to split α_1-AT (Zhu & Chan, 1987).

In earlier studies, the stabilization of split α_1-AT has generally been discussed in terms of the localized relief of strain caused by cleavage of the Met358–Ser359 bond within a stressed surface-exposed polypeptide loop (Löbermann et al., 1984; Carrell & Travis, 1985; Carrell & Owen, 1985; Bruch et al., 1988), although Löbermann et al. (1984) have noted that strain in a molecule is generally thought to be distributed

throughout the whole structure. In this study, the large changes in the spectral properties of the polypeptide backbone that are observed by FT-IR spectroscopy can be directly assigned to the formation of well-defined hydrogen bonds in α-helices and β-sheets in split α_1-AT. The magnitude of these changes for two forms of a water-soluble protein measured under physiological conditions is unusual. Our data suggest that split α_1-AT is stabilized relative to the native form by a more complete hydrogen bonding of its secondary structure (particularly α-helical). The lability of the native serpin structure is consequent on a far more extensive degree of stress than has previously been supposed.

ACKNOWLEDGMENTS

We thank the Wellcome Trust for support and the Science and Engineering Research Council for beamtime at the Institut Laue Langevin, Grenoble. We are grateful to Dr. J. Feeney and Dr. C. Bauer for use of the 400-MHz ^{1}H NMR spectrometer at the National Institute of Medical Research, Mill Hill, London, and Dr. A. de Geyer for support at ILL.

REFERENCES

Bruch, M., Weiss, V., & Engel, J. (1988) *J. Biol. Chem. 263*, 16626–16630.
Carrell, R. W., & Owen, M. C. (1985) *Nature 317*, 730–732.
Carrell, R., & Travis, J. (1985) *Trends Biochem. Sci. 10*, 20–24.
Conrad, H., Mayer, A., Thomas, H. P., & Vogel, H. (1969) *J. Mol. Biol. 41*, 225–229.
Gettins, P., & Harten, B. (1988) *Biochemistry 27*, 3634–3639.
Ghosh, R. E. (1989) Internal Publication 89GH02T, Institut Laue Langevin, Grenoble, France.
Glatter, O., & Kratky, O. (1982) in *Small Angle X-ray Scattering*, Academic Press, London.
Haris, P. I., Lee, D. C., & Chapman, D. (1986) *Biochim. Biophys. Acta 874*, 255–265.
Kauppinen, J. K., Moffatt, D. J., Mantsch, H. H., & Cameron, D. G. (1981) *Appl. Spectrosc. 35*, 271–276.
Lee, D. C., & Chapman, D. (1986) *Biosci. Rep. 6*, 235–256.
Löbermann, D., Tokuoka, R., Deisenhofer, J., & Huber, R. (1984) *J. Mol. Biol. 177*, 531–556.
Mantsch, H. H., Surewicz, W. K., Muga, A., Moffatt, D. J., & Casal, H. L. (1989) Proceedings of the 7th International Conference on FT-IR Spectroscopy, Fairfax, Canada.
McDonald, R. C., Steiz, T. A., & Engelman, D. M. (1979) *Biochemistry 18*, 338–342.
Moody, M. F., Vachette, P., & Foote, A. M. (1979) *J. Mol. Biol. 133*, 517–532.
Olinger, J. M., Hill, D. M., Jakobsen, R. J., & Broody, R. S. (1986) *Biochim. Biophys. Acta 869*, 89–98.
Perkins, S. J. (1988a) *Biochem. J. 254*, 313–327.
Perkins, S. J. (1988b) *New Compr. Biochem. 18B* (Part II), 143–264.
Perkins, S. J., Haris, P. I., Sim, R. B., & Chapman, D. (1988) *Biochemistry 27*, 4004–4012.
Perkins, S. J., Nealis, A. S., & Sim, R. B. (1990) *Biochemistry 29*, 1167–1175.
Smith, K. F., Harrison, R. A., & Perkins, S. J. (1990) *Biochem. J.* (in press).
Surewicz, W. K., & Mantsch, H. H. (1988) *Biochim. Biophys. Acta 952*, 115–130.
Susi, H., & Byler, D. M. (1986) *Methods Enzymol. 130*, 290–311.
Zhu, X.-J., & Chan, S. K. (1987) *Biochem. J. 246*, 19–23.

Primary Intermediate in the Reaction of Mixed-Valence Cytochrome *c* Oxidase with Oxygen

Sanghwa Han,‡ Yuan-chin Ching, and Denis L. Rousseau*
AT&T Bell Laboratories, Murray Hill, New Jersey 07974
Received November 15, 1989; Revised Manuscript Received December 18, 1989

ABSTRACT: The reaction of dioxygen with mixed-valence cytochrome *c* oxidase was followed in a rapid-mixing continuous-flow apparatus. The optical absorption difference spectrum and a kinetic analysis confirm the presence of the primary oxygen intermediate in the 0–100-μs time window. The resonance Raman spectrum of the iron–dioxygen stretching mode (568 cm^{-1}) supplies evidence that the degree of electron transfer from the iron atom to the dioxygen is similar to that in oxy complexes of other heme proteins. Thus, the Fe–O_2 bond does not display any unique structural features that could account for the rapid reduction of dioxygen to water. Furthermore, the frequency of the iron–dioxygen stretching mode is the same as that of the primary intermediate in the fully reduced enzyme, indicating that the oxidation state of cytochrome *a* plays no role in controlling the initial properties of the oxygen binding site.

Cytochrome *c* oxidase (CcO), the terminal enzyme in the electron transport chain, transfers four electrons to dioxygen to reduce it to water. This process involves the generation of several intermediates in a very complex series of changes. Until now, it has been difficult to identify and follow the progress of these intermediates at physiological temperatures owing to their short lifetimes coupled with difficulties in detecting them spectroscopically. Reliance was made primarily on the optical absorption difference spectrum. Recently, preliminary resonance Raman spectra have been obtained on some of the early intermediates (Babcock et al., 1984, 1985;

‡Partially supported by Grant GM-39359 from the National Institute for General Medical Sciences.

0006-2960/90/0429-1380$02.50/0